Generic electron mobility in surface states on thin helium films

E. Krotscheck[1,*] and M. D. Miller[1,2,†]
[1]*Institut für Theoretische Physik, Johannes-Kepler-Universität, A-4040 Linz, Austria*
[2]*Department of Physics and Astronomy, Washington State University, Pullman, Washington 99164-2814, USA*
(Received 26 June 2006; revised manuscript received 29 December 2006; published 30 May 2007)

We study the mobility of electrons adsorbed on thin ^{4}He films on flat, uniform, dielectric substrates. Utilizing the time-dependent version of the Euler-Lagrange, hypernetted chain variational theory, we compute the inelastic scattering rate of an electron due to collisions with film excitations (third sound). We obtain an analytic result valid in the long-wavelength limit. In agreement with experiment, the mobility shows oscillations due to the underlying transverse film structure. The oscillations are due to the explicit appearance of the third sound speed in the scattering rate, since the third sound speed itself oscillates in conjunction with the ^{4}He film structure. The calculated mobilities tend to be higher than reported mobilities on thin films. We attribute this difference to the contribution to the mobility from substrate structure and defects that are omitted in this model. We interpret our results as *generic* mobilities that are valid in the limit of perfectly smooth, structureless substrates.

DOI: 10.1103/PhysRevB.75.205440 PACS number(s): 67.70.+n, 67.60.Fp, 64.30.+t

I. INTRODUCTION

In this paper, we examine the physics of electrons physisorbed on the surface of thin helium films, in particular, those aspects that relate to the interaction of the electron with the low-lying excitations of the helium. Our objective is to introduce a first-principles theory for the electron mobility and compare the predictions with existing experimental data. This section shall comprise a very brief summary of the experimental and theoretical background concerning the study of electrons and their interaction with a dynamic liquid helium surface. We stress that the following material is not meant to be an exhaustive review of the field, but simply a summary of those aspects of the existing experimental and theoretical results that we feel form the background for the present study.

In 1964, Sommer[1] showed that there exists an appreciable barrier (on the order of 1 eV) for electron injection through a helium surface. Cole and Cohen[2] and Cole[3] pointed out that the external, attractive electrostatic image potential coupled with the large repulsion localized at the helium surface would create a potential well that could trap the electron on the helium surface. In 1972, Brown and Grimes[4] reported mobilities in basic agreement with the measurements of Ref. 5 and the calculations of Ref. 3. The reported mobilities were on the order of 10^4–10^5 cm^2/V s at temperatures presumably in the range 1.2–1.5 K. These mobilities are in the regime dominated by scattering from helium vapor.

As the temperature is lowered, the vapor density becomes small and the electron mobility increases. It eventually becomes limited by scattering from helium surface excitations (ripplons) and is independent of temperature. This possibility was first pointed out by Cole.[3] The ripplon-limited asymptotic regime was seen by Rybalko *et al.*,[6] Grimes and Adams,[7] and Bridges and McGill.[8] However, as pointed out in Ref. 8, there is a spread of about a factor of 50 in the reported values of the ripplon-limited mobility.

Following a suggestion by Gor'kov and Chernikova,[9,10] Wanner and Leiderer[11] showed that at a critical value of an applied electric field, the surface excitation spectrum becomes soft and unstable. This phenomenon can also be driven by electron density, and at zero applied field, it determines a maximum allowable surface electron density. Ikezi and Platzman[12] then suggested that for a thin film, the instability would occur at a higher electron density than for the free helium surface because of the change in the helium surface excitation spectrum. For a thin film, the restoring force is the substrate van der Waals interaction (third sound) whose spectrum is linear in the wave vector k, whereas for the free surface, the restoring force is basically surface tension whose spectrum goes like $k^{3/2}$. In agreement with theoretical predictions, Etz *et al.*[13] demonstrated greatly increased maximum electron surface density, on the order of 10^{11} cm^{-2}, for absorption on a helium film with either insulating or conducting substrates. The first thin helium film experiment was probably that reported by Kajita and Sasaki[14] for a helium film on a neon substrate. These authors worked at an electron density of approximately 7×10^8 cm^{-2} and searched unsuccessfully for a localization transition, that is, a rapid decrease in the mobility due to the formation of a polaron.

Paalanen and Iye[15] looked at electron mobility on a bare H_2 substrate and also one with a thin (unsaturated) helium film. They explained a mobility minimum that occurs in the very thin film regime (the immobile helium) as due to the interplay between stiffening of the film modes in the zero thickness limit and decrease in the image field for thicker films. Most interestingly, they also reported an additional pair of oscillations in the lowest-temperature sample (1.45 K) that they attributed to *layer formation* in the mobile helium film. The mobilities were on the order of 10^3 cm^2/V s.

In 1987, Cieslikowski *et al.*[16] reported mobility measurements for ^{3}He and ^{4}He films on a H_2 substrate. This experiment extended the work of Ref. 15 to thicker helium films. The authors stated that they were looking for a transition from thin-film mobilities to thick-film mobilities. Surprisingly, they found instead additional oscillations in the mobility that they attributed to layering in the mobile film. The

 ©2007 The American Physical Society

mobilities were again in the range of 10^3 cm^2/V s. The remarkable aspect of these data is that they show (at 2.5 K) evidence for at least nine oscillations in the mobility, implying physical layering in the helium film extending quite far from the solid substrate. We note that this result is in marked contrast to adsorption isotherm[17] and superfluid fraction[18] measurements, which sense only three or four layers. The authors also noted that a ^{3}He sample displayed qualitatively similar modulations. However, as pointed out by Shikin *et al.*, [19] there is a many orders of magnitude difference between free-surface (ripplon-limited) mobilities and thin-film mobilities. Indeed, Shirahama *et al.*[20] report ^{4}He free-surface, ripplon-limited mobilities on the order of 10^7-10^8 cm^2/V s. Building on a previous model introduced by Monarkha *et al.*,[21] the authors of Ref. 19 argue that the mobilities being measured in the thin-film experiments may be dominated by surface impurities or inhomogeneities.

Theoretical support for the important role played by substrate inhomogeneities and defects in determining the electron mobility on helium films can be found in the work of Studart and co-workers.[22–24] In particular, in Ref. 22, this group reports electron mobilities on a H_2 substrate on the order of 10^4 cm^2/V s for a choice of potential parameters that yield results in agreement with experiment. In contrast, they also studied electron mobilities on ^{3}He-^{4}He mixture films (no solid substrate) and report mobilities on the order of 10^8-10^9 cm^2/V s for systems with no holding field and at the lowest temperatures.

From this concise history, a number of salient facts begin to emerge. First, there is a many orders of magnitude difference between the measured electron mobilities on the free helium surface and on the surface of thin films. Second, there is a fairly large spread in measured mobilities from different experiments. Finally, there is evidence that for thin films, the mobility is strongly affected by substrate inhomogeneities and defects.

In this paper, we address a specific aspect of the experimental electron mobility, namely, the oscillations found by Cieslikowski *et al.*[16] and their correlation with the layering in the mobile film. In particular, we want to explain why electron mobilities are highly sensitive to the layer structure, whereas other experiments such as adsorption isotherms[17] and the superfluid fraction[18] are not. For that purpose, we shall present a manifestly microscopic calculation of the helium contribution to the electron mobility on thin ^{4}He films. Our calculations are based on the time-dependent, variational theory developed for inhomogeneous, strongly interacting boson systems.[25] Technically, we introduce the concept of time-dependent *pair* fluctuations. We provide a microscopic definition of a *transport current*, as the expectation value of the current operator evaluated to second order in the fluctuating part of the wave function. This leads to the derivation of elastic and inelastic currents. The energy loss of the electron is identified with the damped part of the inelastic current. We also show how the concept of fluctuating pair correlations is essential in obtaining both a nontrivial effective mass and inelastic processes.

It is well understood[25] that the helium film profile develops oscillations in density that are similar to layer formation in a solid film. This layering is then reflected in many properties of the film including the excitation spectrum.[26,27] Relevant to the case of electron mobility is, as we shall see, the nonmonotonic behavior of the speed of third sound that goes through a series of oscillations in sync with liquid layer formation as the film grows. Typically, the speed of sound has a maximum at layer completion. We derive an explicit result for the electron mobility. We can clearly separate the contribution to the inelastic current into a smooth background contribution due to elastic scattering off of high-lying helium excitations and an oscillatory part coming from coupling to surface excitations. The latter part oscillates, in agreement with experiment, with the ^{4}He film thickness through the explicit appearance of the third sound speed. We will show *how* these oscillations affect the electron mobility and *why* this quantity is particularly sensitive against even small fluctuations in speed of the surface excitation.

We refer to our calculated mobilities as *generic* since the calculated electron scattering only includes coupling to the excitations of the helium film (dominated by sound quanta) and a uniform, perfectly flat dielectric substrate. We do not include contributions to electron scattering from substrate corrugation and substrate defects.

Our numerical results for the generic mobilities are reported for a series of values of the substrate dielectric constant, $\epsilon_S=3-5$, that are in the range appropriate for a glass substrate. This ensures that this calculation is consistent with our previous microscopic calculations of the third sound spectra. We note that the thin helium film experiments have been reported only for a H_2 substrate. Our generic mobilities for the glass substrate are 1–2 orders of magnitude larger than the magnitudes of the mobilities reported on the H_2 substrate. We will suggest that, in line with the explanation of Ref. 19, most of the disparity may be due to the neglected effects of scattering due to substrate defects and inhomogeneities.

In Sec. II, we discuss the aspects of the theory necessary to calculate scattering times for impurities adsorbed in a ^{4}He film. Technically, we have to deal with two tasks: One is the calculation of coupling matrix elements between the electrons and the ^{4}He atoms, the other one is the calculation of inelastic-scattering processes *inside* the medium. The case at hand is simplified by the fact that the physics is dominated by the long-wavelength properties of the electron-helium coupling. This will permit a number of significant simplifications and allow us to express the essential physics solely in terms of physical observables such as the ^{4}He speed of sound and the coverage dependence of the electron binding energy. The necessary derivations are presented in Secs. III and IV. In particular, we will derive there the result that displays clearly the reason for why electron mobility measurements are sensitive to the layer structure of the film. In Sec. V, we show our numerical results and compare them with experiment. Section VI is the conclusion. In the Appendix, we derive various results in the limit of an infinitely thick helium film and discuss some of the subtleties involved with that limit.

II. GROUND STATE AND EXCITATIONS

A. Energetics and structure

The microscopic description of static and dynamic properties of helium films, including the dynamics of impurities,

has been described in various papers,[28–31] and the reader is referred to these papers for general concepts and definitions. The background ^{4}He film is described by a Hamiltonian

$$H_N = \sum_i \left[-\frac{\hbar^2}{2m_4}\nabla_i^2 + U_{\rm sub}(\mathbf{r}_i) \right] + \sum_{i<j} V(|\mathbf{r}_i - \mathbf{r}_j|), \quad (2.1)$$

where $V(|\mathbf{r}_i - \mathbf{r}_j|)$ is the ^{4}He–^{4}He interaction, and $U_{\rm sub}(\mathbf{r})$ is the external "substrate" potential. The ground-state wave function is written in the Jastrow-Feenberg form as

$$\Psi_N(\mathbf{r}_1, \ldots, \mathbf{r}_N) = \exp \frac{1}{2}\left[\sum_i u_1(\mathbf{r}_i) + \sum_{i<j} u_2(\mathbf{r}_i, \mathbf{r}_j) + \sum_{i<j<k} u_3(\mathbf{r}_i, \mathbf{r}_j, \mathbf{r}_k) \right]. \quad (2.2)$$

An essential part of the approach is the *optimization* of the many-body correlations by solving the Euler equations

$$\frac{\delta E_N}{\delta u_n(\mathbf{r}_1, \ldots, \mathbf{r}_n)} = 0 \quad (n = 1,2,3), \quad (2.3)$$

where E_N is the energy expectation value of the N-particle Hamiltonian [Eq. (2.1)] with respect to the wave function [Eq. (2.2)]. Executing the variations and manipulating the Euler equations to bring them into a numerically tractable form lead to an effective one-body Schrödinger equation

$$\left[-\frac{\hbar^2}{2m_4}\nabla^2 + U_{\rm ext}(\mathbf{r}) + V_H(\mathbf{r}) \right] \sqrt{\rho_1(\mathbf{r})} = \mu_4 \sqrt{\rho_1(\mathbf{r})} \quad (2.4)$$

for the one-body density $\rho_1(\mathbf{r})$ and the ^{4}He chemical potential μ_4, where $V_H(\mathbf{r})$ is a self-consistently determined "Hartree" potential. Optimization of the two-body correlations leads to a normal mode equation as follows:

$$\int d^3r' H_1(\mathbf{r})[H_1(\mathbf{r})\delta(\mathbf{r}-\mathbf{r}') + 2\tilde{V}_{p\text{-}h}(\mathbf{r},\mathbf{r}')]\phi^{(m)}(\mathbf{r}') = (\hbar\omega_m)^2 \phi^{(m)}(\mathbf{r}), \quad (2.5)$$

where

$$H_1(\mathbf{r}) = -\frac{\hbar^2}{2m_4}\nabla^2 + U_{\rm ext}(\mathbf{r}) + V_H(\mathbf{r}) - \mu_4 = -\frac{\hbar^2}{2m_4}\frac{1}{\sqrt{\rho_1(\mathbf{r})}}\nabla\,\rho_1(\mathbf{r})\cdot\nabla\frac{1}{\sqrt{\rho_1(\mathbf{r})}}, \quad (2.6)$$

and

$$\tilde{V}_{p\text{-}h}(\mathbf{r},\mathbf{r}') = \sqrt{\rho_1(\mathbf{r})}V_{p\text{-}h}(\mathbf{r},\mathbf{r}')\sqrt{\rho_1(\mathbf{r}')}, \quad (2.7)$$

is the "particle-hole interaction" that is determined self-consistently within the variational theory. In an exact theory, the particle-hole interaction can also be defined through

$$V_{p\text{-}h}(\mathbf{r},\mathbf{r}') = \frac{\delta V_H(\mathbf{r})}{\delta\rho_1(\mathbf{r}')}. \quad (2.8)$$

For our purposes, it is important to know that the eigenfunctions $\phi^{(m)}(\mathbf{r}')$ can be identified with the physical density fluctuations within a Feynman theory of excitations of the liquid.

The Hamiltonian of the $N+1$ particle system consisting of N ^{4}He atoms and one impurity (an electron in our case) located at $\mathbf{r}_0$ is

$$H_{N+1}^{(I)} = -\frac{\hbar^2}{2m_I}\nabla_0^2 + U_{\rm sub}^{(I)}(\mathbf{r}_0) + \sum_{i=1}^{N} V^{(I)}(|\mathbf{r}_0 - \mathbf{r}_i|) + H_N. \quad (2.9)$$

The variational wave function [Eq. (2.2)] for an inhomogeneous N-particle Bose system with a single impurity atom is

$$\Psi_{N+1}^{(I)}(\mathbf{r}_0,\mathbf{r}_1,\ldots,\mathbf{r}_N) = \exp\frac{1}{2}\left[u_1^{(I)}(\mathbf{r}_0) + \sum_{1\leqslant i\leqslant N} u_2^{(I)}(\mathbf{r}_0,\mathbf{r}_i) + \cdots \right]\Psi_N(\mathbf{r}_1,\ldots,\mathbf{r}_N). \quad (2.10)$$

Analogous to Eq. (2.4), the impurity one-body density is determined by a one-body Schrödinger equation in terms of an effective Hartree potential,

$$\left[-\frac{\hbar^2}{2m_I}\nabla_0^2 + U_{\rm sub}^{(I)}(\mathbf{r}_0) + V_H^{(I)}(\mathbf{r}_0) \right]\sqrt{\rho_1^{(I)}(\mathbf{r}_0)} = \mu_I\sqrt{\rho_1^{(I)}(\mathbf{r}_0)}, \quad (2.11)$$

for the impurity density $\rho_1^{(I)}(\mathbf{r}_0)$ and the impurity binding energy μ_I. Similar to Eq. (2.6) it is convenient to introduce the one-body operator

$$H_1^{(I)}(\mathbf{r}_0) = -\frac{\hbar^2}{2m_I}\nabla_0^2 + U_{\rm ext}^{(I)}(\mathbf{r}_0) + V_H^{(I)}(\mathbf{r}_0) - \mu_I = -\frac{\hbar^2}{2m_I}\frac{1}{\sqrt{\rho_1^{(I)}(\mathbf{r}_0)}}\nabla\,\rho_1^{(I)}(\mathbf{r}_0)\cdot\nabla\frac{1}{\sqrt{\rho_1^{(I)}(\mathbf{r}_0)}} \quad (2.12)$$

and to use it to generate a basis of impurity wave functions

$$H_1^{(I)}(\mathbf{r}_0)\,\eta^{(\alpha)}(\mathbf{r}_0) = \varepsilon_\alpha \eta^{(\alpha)}(\mathbf{r}_0). \quad (2.13)$$

The spectrum is ε_α and the set of states are the $\{\eta^{(\alpha)}(\mathbf{r}_0)\}$. In the following, we will label impurity states with Greek letters and the background phonons with Latin letters.

We also need the two-body equation because it contains the basic ingredients needed for the dynamics of the system. The pair equation is a relationship between a particle-hole interaction $\tilde{V}_{p\text{-}h}^{(I)}(\mathbf{r}_0,\mathbf{r}')$ and the "direct correlation function" $\tilde{X}^{(I)}(\mathbf{r}_0,\mathbf{r}')$ that is best written in a matrix representation in terms of the states $\phi^{(m)}$ and $\eta^{(\alpha)}$,

$$(\eta^{(\alpha)}|\tilde{X}^{(I)}|\phi^{(m)}) = -2\frac{(\eta^{(\alpha)}|\tilde{V}_{p\text{-}h}^{(I)}|\phi^{(m)})}{\varepsilon_\alpha + \hbar\omega_m}, \quad (2.14)$$

where the impurity particle-hole interaction is, in an exact theory, given by

$$\tilde{V}_{p\text{-}h}^{(I)}(\mathbf{r}_0,\mathbf{r}_1) = \sqrt{\rho_1^{(I)}(\mathbf{r}_0)}V_{p\text{-}h}^{(I)}(\mathbf{r}_0,\mathbf{r}_1)\sqrt{\rho_1(\mathbf{r}_1)} = \sqrt{\rho_1^{(I)}(\mathbf{r}_0)}\frac{\delta V_H^{(I)}(\mathbf{r}_0)}{\delta\rho(\mathbf{r}_1)}\sqrt{\rho_1(\mathbf{r}_1)}. \quad (2.15)$$

B. Excitations and linear response

Excitations and the response to perturbations are treated analogously within the theory. The system is exposed to a weak, time-dependent external perturbation $\Sigma_i U_{\rm ext}(\mathbf{r}_i;t)$. As a response, the wave function becomes time dependent. The natural generalization of the variational approach to excited states is to allow for *time-dependent* correlations $u_n(\mathbf{r}_0,\ldots,\mathbf{r}_n;t)$ of the form

$$\Phi(t) = \frac{1}{\sqrt{\langle\Psi^I|\Psi^{(I)}\rangle}} e^{-iE^{(I)}_{N+1}t/\hbar}\Psi^{(I)}(\mathbf{r}_0,\mathbf{r}_1,\ldots\mathbf{r}_N;t), \tag{2.16}$$

where $\Psi^{(I)}(\mathbf{r}_0,\mathbf{r}_1,\ldots\mathbf{r}_N;t)$ contains the dynamic, time-dependent correlations. These are again written in a Jastrow-Feenberg form as

$$\Psi^{(I)}(\mathbf{r}_0,\mathbf{r}_1,\ldots,\mathbf{r}_N;t) = \exp\left[\frac{1}{2}\delta U(\mathbf{r}_0,\mathbf{r}_1,\ldots\mathbf{r}_N;t)\right] \times\Psi^{(I)}_{N+1}(\mathbf{r}_0,\mathbf{r}_1,\ldots,\mathbf{r}_N), \tag{2.17}$$

$$\delta U(\mathbf{r}_0,\mathbf{r}_1,\ldots,\mathbf{r}_N;t) = \delta u_1(\mathbf{r}_0;t) + \sum_{1\leqslant i\leqslant N}\delta u_2(\mathbf{r}_0,\mathbf{r}_i;t). \tag{2.18}$$

The time-dependent parts of the correlations, $\delta U(\mathbf{r}_0,\mathbf{r}_1,\ldots,\mathbf{r}_N;t)$, are determined by the stationary principle

$$\delta\mathcal{S} = \delta\int_{t_0}^{t_1}\mathcal{L}(t)dt = \delta\int_{t_0}^{t_1}\left\langle\Phi(t)\left|H^{(I)}_{N+1} - i\hbar\frac{\partial}{\partial t}\right|\Phi(t)\right\rangle dt = 0. \tag{2.19}$$

The variations of the action integral with respect to the excitation amplitudes $\delta u_1^*(\mathbf{r}_0;t)$ and $\delta u_2^*(\mathbf{r}_0,\mathbf{r}_1;t)$ lead to coupled one- and two-particle continuity equations for the *first-order* density fluctuations. In the general impurity theory,[30] it was shown that the equation of motion can be written in the form of a nonlinear eigenvalue problem as

$$\hbar\omega r_{\boldsymbol{\alpha}} = \sum_{\boldsymbol{\beta}}[\delta_{\boldsymbol{\alpha\beta}}\varepsilon_{\boldsymbol{\alpha}} + \Sigma_{\boldsymbol{\alpha\beta}}(\omega)]r_{\boldsymbol{\beta}}, \tag{2.20}$$

where the $r_{\boldsymbol{\alpha}}$ are the expansion coefficients of the time (or frequency-) dependent part of the impurity wave function in terms of the states $\eta^{(\alpha)}(\mathbf{r}_0)$, and

$$\Sigma_{\boldsymbol{\alpha\beta}}(\omega) = -\sum_{\boldsymbol{\gamma m}}\frac{W^{*(\boldsymbol{\alpha})}_{\boldsymbol{\gamma m}}W^{(\boldsymbol{\beta})}_{\boldsymbol{\gamma m}}}{\hbar\omega_{\boldsymbol{m}} + \varepsilon_{\boldsymbol{\gamma}} - \hbar\omega} \tag{2.21}$$

is the impurity's self-energy. The impurity-impurity-phonon vertex function occurring in the self-energy [Eq. (2.21)] is[30]

$$W^{(\boldsymbol{\alpha})}_{\boldsymbol{\gamma m}} = \frac{1}{2}\int d^3r_0\frac{\eta^{(\boldsymbol{\alpha})}(\mathbf{r}_0)\eta^{*(\gamma)}(\mathbf{r}_0)}{\sqrt{\rho^{(I)}_1(\mathbf{r}_0)}}[\varepsilon_{\boldsymbol{\gamma}} - \varepsilon_{\boldsymbol{\alpha}} - H^{(I)}_1(\mathbf{r}_0)]\widetilde{X}_{\boldsymbol{m}}(\mathbf{r}_0)$$
$$= -\frac{\hbar^2}{2m_I}\int d^3r_0\,\eta^{*(\gamma)}(\mathbf{r}_0)\sqrt{\rho^{(I)}_1(\mathbf{r}_0)}\,\nabla X_{\boldsymbol{m}}(\mathbf{r}_0)\cdot\nabla\frac{\eta^{(\boldsymbol{\alpha})}(\mathbf{r}_0)}{\sqrt{\rho^{(I)}_1(\mathbf{r}_0)}}, \tag{2.22}$$

$$X_{\boldsymbol{m}}(\mathbf{r}_0) \equiv \int d^3r_1 X^{(I)}(\mathbf{r}_0,\mathbf{r}_1)\sqrt{\rho_1(\mathbf{r}_1)}\phi^{(\boldsymbol{m})}(\mathbf{r}_1). \tag{2.23}$$

The three-body vertex function $W^{(\alpha)}_{\boldsymbol{\gamma m}}$ describes an impurity atom scattering off of a background excitation and is given in terms of quantities obtained in the ground-state calculation.

C. Transport currents

The formulation of the theory up to this point provides the material for calculating impurity motion. However, For the problem at hand, we must introduce yet another quantity, namely, the *second-order current.* The flux of impurities (here, specifically, electrons) is given by the expectation value of the current operator

$$\hat{\mathbf{j}}^{(I)}(\mathbf{r}) = \frac{1}{2m_I}\left(\frac{\hbar}{\mathrm{i}}\nabla_0\delta(\mathbf{r}_0-\mathbf{r}) + \delta(\mathbf{r}_0-\mathbf{r})\frac{\hbar}{\mathrm{i}}\nabla_0\right), \tag{2.24}$$

with respect to the wave function [Eqs. (2.17) and (2.18)]. This expectation value must be calculated to *second order* in the fluctuating correlations $\delta u_n(\mathbf{r}_1,\ldots,\mathbf{r}_n;t)$ because the first-order term is periodic in time and does not lead to mass transport; thus,

$$\mathbf{j}^{(I)}_2(\mathbf{r}) \equiv \frac{1}{4}\frac{\langle\Psi_0|\delta U^*\hat{\mathbf{j}}^{(I)}(\mathbf{r})\delta U|\Psi_0\rangle}{\langle\Psi_0|\Psi_0\rangle}. \tag{2.25}$$

The excitation operator $\delta U(t)$ is understood to be obtained from the *first- order* equations of motion [Eq. (2.19)]. One finds[32]

$$\mathbf{j}^{(I)}_2(\mathbf{r}_0) = \mathrm{Re}\,\frac{\hbar}{4m_I\mathrm{i}}\Big[\delta\rho^{*(I)}_1(\mathbf{r}_0;t)\,\nabla\,\delta u_1(\mathbf{r}_0;t) + \int d^3r_1\,\delta\rho^{*(I)}_2(\mathbf{r}_0,\mathbf{r}_1;t)\nabla_0\delta u_2(\mathbf{r}_0,\mathbf{r}_1;t)\Big], \tag{2.26}$$

where $\delta\rho^{(I)}_i$ are the density fluctuations to first order. The *general* second-order impurity current involves the three-body distribution functions; a tractable form can be derived within the same scheme that led in Sec. II B to the first-order equations of motion:

$$\mathbf{j}^{(I)}_2(\mathbf{r}_0) = \mathrm{Re}\,\frac{\hbar}{4m_I\mathrm{i}}\Big[\varphi^*_\omega(\mathbf{r}_0;t)\,\nabla\,\varphi_\omega(\mathbf{r}_0;t) + \int d^3r_1d^3r_2S(\mathbf{r}_1,\mathbf{r}_2)\delta\widetilde{u}^*_2(\mathbf{r}_0,\mathbf{r}_1)\nabla_0\delta\widetilde{u}_2(\mathbf{r}_0,\mathbf{r}_2)\Big]$$
$$\equiv \mathbf{j}^{(I)}_{2,\mathrm{el}}(\mathbf{r}_0) + \mathbf{j}^{(I)}_{2,\mathrm{inel}}(\mathbf{r}_0). \tag{2.27}$$

Here, $S(\mathbf{r}_1,\mathbf{r}_2)$ is background static structure function. $\varphi_\omega(\mathbf{r}_0)$ is the electron wave function that was obtained from the effective Schrödinger equation [Eq. (2.20)] and can, evidently, be identified with the elastic channel wave function. The form of Eq. (2.27) gives the decomposition of the current into a one-body term, which describes the *elastic* channels, and a many-body term contributing to *inelastic* scattering. The latter term contains the fluctuating pair correlations

$\delta u_2(\mathbf{r},\mathbf{r}_2)$, which demonstrates the importance of time-dependent pair correlations for describing inelastic processes. Using the two-body equations of motion, we can express the inelastic current as

$$\mathbf{j}^{(I)}_{2,\mathrm{inel}}(\mathbf{r}_0;t) = \frac{\hbar}{4m_I}\,\mathrm{Im}\left[\sqrt{\rho_1^{(I)}(\mathbf{r}_0)}\sum_{\gamma}\eta^*_{\gamma}(\mathbf{r}_0)\,\nabla\,\frac{\eta_{\gamma}(\mathbf{r}_0)}{\sqrt{\rho_1^{(I)}(\mathbf{r}_0)}}\right.$$
$$\left.\times\sum_{m}\frac{W^{*(\alpha)}_{\gamma m}W^{(\beta)}_{\gamma m}r^*_{\alpha}r_{\beta}}{|\varepsilon_{\gamma}+\hbar\omega_m-\hbar\omega+i\epsilon|^2}\right], \tag{2.28}$$

where the r_β are the amplitudes of the electron in the individual single-particle states, cf. Eq. (2.20).

Equation (2.28) also demonstrates why we identify the second term in Eq. (2.27) with an inelastic current. If the self-energy [Eq. (2.21)] is complex, the current [Eq. (2.28)] has a double pole and the expression must be reinterpreted as a rate equation.

III. ELECTRON: SELF-ENERGY

The problem at hand differs from the previously studied problem of atomic impurities in the important aspect that the most visible effect, namely, the oscillatory behavior of the electron mobility as a function of the film thickness, can be explained by looking at long-wavelength expansions for all quantities involved. This does not necessarily imply that other contributions are negligible; all we say is that these can, at most, contribute a smooth background.

We assume that the system fills a box of area L^2 with the z axis oriented transversly to the substrate. The substrate fills the lower half space. The ^{4}He *coverage* n is defined by $n=N/L^2=(1/L^2)\int d^3r\rho_1(\mathbf{r})$. In the plane surface geometry, the electron single-particle basis functions, Eq. (2.13), have the form

$$\eta^{(\boldsymbol{\alpha})}(\mathbf{r}_0) = \eta^{(\alpha)}(z)e^{i\mathbf{q}_\parallel\cdot\mathbf{r}}, \tag{3.1}$$

and the corresponding energies are

$$\varepsilon_{\boldsymbol{\alpha}} = \epsilon_\alpha + \frac{\hbar^2\mathbf{q}_\parallel^2}{2m_I}, \tag{3.2}$$

where $\eta^{(\alpha)}(z)$ and the ϵ_α are the eigenfunction-eigenvalue pairs of Eq. (2.13) for $q_\parallel=0$.

We may assume that the electron remains in its transverse ground state but has a parallel momentum and that transitions to intermediate phonon states are negligible, i.e., we keep only

$$\eta^{(o,\mathbf{q}_\parallel)}(\mathbf{r}_0) = \frac{1}{L}\sqrt{\rho_1^{(I)}(z)}e^{i\mathbf{q}_\parallel\cdot\mathbf{r}}, \tag{3.3}$$

$\varepsilon_0=\hbar^2q_\parallel^2/2m_I$, and the third sound mode is labeled by ($\mathbf{m}\rightarrow(R,\mathbf{q}_R)$). In this limit we obtain

$$W^{(o,\mathbf{q}_\parallel)}_{(o,\mathbf{q}_\gamma)(R,\mathbf{q}_R)} = -\frac{\hbar^2}{2m_IL^2}\int d^3r_0\rho_1^{(I)}(z)e^{-i\mathbf{q}_\gamma\cdot\mathbf{r}_\parallel}\,\nabla X_R(\mathbf{r}_0)\cdot\nabla e^{i\mathbf{q}_\parallel\cdot\mathbf{r}_\parallel}$$
$$= \frac{\hbar^2}{2m_IL}\delta_{\mathbf{q}_R+\mathbf{q}_\parallel-\mathbf{q}_\gamma}\mathbf{q}_R\cdot\mathbf{q}_\parallel\int dz_0\rho_1^{(I)}(z_0)X_R(z_0,q_R)$$
$$\equiv \frac{\hbar^2}{2m_IL}\delta_{\mathbf{q}_R+\mathbf{q}_\parallel-\mathbf{q}_\gamma}\mathbf{q}_R\cdot\mathbf{q}_\parallel X_{o,R}(q_R). \tag{3.4}$$

If transitions to higher-lying electron and phonon states are negligible, we can restrict the summation over intermediate states to the lowest (third sound) excitation and write the self-energy as

$$\Sigma(q_\parallel,\omega)\equiv\Sigma_{(o,\mathbf{q}_\parallel),(o,\mathbf{q}_\parallel)}(\omega)$$
$$= -\sum_{\mathbf{q}_\gamma\mathbf{q}_R}\frac{|W^{(o,\mathbf{q}_\parallel)}_{(o,\mathbf{q}_\gamma),(R,\mathbf{q}_R)}|^2}{\hbar\omega_R(q_R)+\frac{\hbar^2}{2m_I}q_\gamma^2-\hbar\omega}$$
$$= -\left(\frac{\hbar^2}{2m_I}\right)^2\int\frac{d^2q_R}{(2\pi)^2}$$
$$\times\frac{|(\boldsymbol{q}_R\cdot\boldsymbol{q}_\parallel)X_{o,R}(q_R)|^2}{\hbar\omega_R(q_R)+\frac{\hbar^2}{2m_I}(\boldsymbol{q}_R+\boldsymbol{q}_\parallel)^2-\hbar\omega}, \tag{3.5}$$

where $\omega_R(q_R)\rightarrow c_3q_R$ for $q_R\rightarrow 0$ is the ripplon and/or third-sound dispersion relation. The long-wavelength expansion of the ripplon and/or third-sound state $\phi_{R,\mathbf{q}_R}(z)$ has been worked out in Ref. 33. In the limit $\mathbf{q}_R\rightarrow 0$, it factorizes as

$$\phi_{R,\mathbf{q}_R}(z) = -\sqrt{\frac{n\hbar q_R^2}{2m_4\omega_R(q_R)}}\Phi_R(z) = \sqrt{\frac{2n\hbar q_R^2}{m_4\omega_R(q_R)}}\frac{d\sqrt{\rho_1(z)}}{dn}. \tag{3.6}$$

$\Phi_R(z)$ is the shape function of the long-wavelength density fluctuation; we have normalized it such that $\int dz\Phi_R(z)\sqrt{\rho_1(z)}=1$. A useful property of the ripplon and/or third-sound shape function $\Phi_R(z)$ can be derived from the fact that $\tilde{V}^{(I)}_{p\text{-}h}(\mathbf{r}_0,\mathbf{r}')$ is rigorously defined from the variation of the self-consistent one-body potential $V_H^{(I)}(\mathbf{r}_0)$, cf. Eq. (2.15). Hence, we have

$$\int d^3r'V^{(I)}_{p\text{-}h}(\mathbf{r}_0,\mathbf{r}')\frac{d\rho_1(\mathbf{r}')}{dn} = \frac{dV_H^I(\mathbf{r}_0)}{dn} \tag{3.7}$$

as well as

$$\int dz\rho_1^{(I)}(z)\frac{dV_H^I(z)}{dn} = \frac{d\mu_I}{dn}. \tag{3.8}$$

We can therefore work out the long-wavelength limit of the direct correlation function

$$X_{o,R}(q_R) = \sqrt{\frac{2n\hbar q_R^2}{m_4\omega_R(q_R)}}\frac{d\mu_I}{dn}\frac{1}{\hbar\omega_R(q_R)+\frac{\hbar^2}{2m_I}q_R^2}, \quad (3.9)$$

and relate it directly to physical observables. Collecting everything, the electron dispersion relation is given by the implicit equation

$$\hbar\omega(q_\parallel) = \frac{\hbar^2 q_\parallel^2}{2m_I} - \left(\frac{\hbar^2}{2m_I}\right)^2 \int \frac{d^2q_R}{(2\pi)^2} \times \frac{|(\boldsymbol{q}_R\cdot\boldsymbol{q}_\parallel)X_{o,R}(q_R)|^2}{\hbar\omega_R(q_R)+\frac{\hbar^2}{2m_I}(\boldsymbol{q}_R+\boldsymbol{q}_\parallel)^2-\hbar\omega(q_\parallel)}. \quad (3.10)$$

The integral is complex; its imaginary part is related to the lifetime, and its real part to the effective mass. To be a bit more general, we allow for an effective mass in the energy denominator. Such an effective mass should *not* appear in the Euler equation [Eq. (3.9)] because this is a static equation between ground-state properties, whereas the effective mass should be the same in all pieces of the energy denominator, i.e., we also assume that $\hbar\omega(q_\parallel)=\hbar^2q_\parallel^2/2m_I^*$ in Eq. (3.10). Then, the energy denominator becomes

$$\hbar\omega_R(q_R)+\frac{\hbar^2}{2m_I^*}(\boldsymbol{q}_R+\boldsymbol{q}_\parallel)^2-\hbar\omega(q_\parallel) = \hbar c_3 q_R + \frac{\hbar^2}{2m_I^*}q_R^2 + \frac{\hbar^2}{2m_I^*}q_R q_\parallel\cos\theta. \quad (3.11)$$

To get an imaginary part, the energy denominator must become zero somewhere in the integration regime. For that, we need q_R in the range

$$-2q_\parallel - \frac{2m_I^*c_3}{\hbar} \leqslant q_R \leqslant 2q_\parallel - \frac{2m_I^*c_3}{\hbar}, \quad (3.12)$$

which says we can have an imaginary part only if $\hbar q_\parallel/m_I^* > c_3$, or that the speed of the thermal electrons is comparable to the third sound speed. In particular, the self-energy is real in the long-wavelength limit $q_\parallel\to 0$, which determines the effective mass.

Thus, if $\hbar q_\parallel < m_I^*c_3$, the self-energy is real and we get a correction to the spectrum. In that limit, we simply have from Eq. (3.10)

$$\Sigma\left(q_\parallel, \frac{\hbar^2q_\parallel^2}{2m_I^*}\right) = -\frac{\hbar^2q_\parallel^2}{2m_I}\int_0^\infty \frac{dq_R q_R}{4\pi}\frac{\hbar^2q_R^2}{2m_I}\frac{|X_{o,R}(q_R)|^2}{\hbar\omega_R(q_R)+\frac{\hbar^2q_R^2}{2m_I^*}}, \quad (3.13)$$

or an effective-mass ratio

$$\frac{m_I}{m_I^*} = 1 - \int_0^\infty \frac{dq_R q_R}{4\pi}\frac{\hbar^2q_R^2}{2m_I}\frac{|X_{o,R}(q_R)|^2}{\hbar\omega_R(q_R)+\frac{\hbar^2q_R^2}{2m_I^*}}. \quad (3.14)$$

To get a qualitative idea of the dependence of the effective mass on the various physical quantities, we insert the long-wavelength expansion [Eq. (3.9)],

$$\frac{m_I}{m_I^*} = 1 - \frac{1}{2\pi}\frac{m_I}{m_4}\left(n\frac{d\mu_I}{dn}\right)^2\frac{1}{n\hbar^2c_3^2}\left[2\frac{r-1-\log r}{(r-1)^2}\right], \quad (3.15)$$

where $r=m_I/m_I^*$. The term in the square bracket goes to 1 as $r\to 1$, and it falls off for large r; hence, it tends to suppress a large effective mass. Both the numerator and the denominator go to zero in the limit of large film thicknesses. Compared to the decay rate [see Eq. (4.5) below], which contains only one c_3 factor in the denominator, the dependence of the effective mass on the "softness" of the surface is obviously much stronger and can occasionally overcome the mass ratio of m_I/m_4 in front of the effective-mass correction.

The calculation of the electron effective mass has two purposes: one is that the decay rate will be seen to be directly proportional to the square of the effective-mass ratio, a strongly fluctuating mass will therefore also enhance fluctuations of the decay rate, and second, to assess the validity of our theoretical scheme, especially the self-energy expression [Eq. (2.21)]. An effective-mass ratio that is of the order of 1 is necessary for the validity of the approximation [Eq. (2.21)] of the electron self-energy.

IV. ELECTRONS: ENERGY LOSS

We introduce the same approximations on the inelastic currents as before: (1) we keep only the lowest state $\hbar\omega_R(q_R)$ and (2) assume that the electron moves with a wave vector $\boldsymbol{q}_\parallel$ in the lowest state (i.e., we keep only the basis function $\eta_0(\mathbf{r})$ or $r_{\boldsymbol{\alpha}}=\delta_{\boldsymbol{\alpha},0}$). For the sake of generality, we also assume, again, that the electron has an effective mass m_I^*. Then, the inelastic current becomes

$$\mathbf{j}_{2,\mathrm{inel}}^{(l)}(\mathbf{r};t) = \frac{1}{2\hbar L^2}\left(\frac{\hbar^2}{2m_I}\right)^3\rho_1^{(l)}(z)\int\frac{d^2q_R}{(2\pi)^2}(\mathbf{q}_R+\mathbf{q}_\parallel) \times \left|\frac{\mathbf{q}_R\cdot\mathbf{q}_\parallel X_{o,R}(q_R)}{\hbar\omega_R(q_R)+\frac{\hbar^2}{2m_I^*}(\mathbf{q}_R+\mathbf{q}_\parallel)^2-\hbar\omega+\mathrm{i}\epsilon}\right|^2. \quad (4.1)$$

If the electron wave number satisfies the inequality [Eq. (3.12)], the inelastic current has a double pole and must be reinterpreted as giving a *decay rate*

$$\lim_{\epsilon\to 0+}\frac{d}{dt}\mathbf{j}^{(I)}_{2,\mathrm{inel}}(\mathbf{r};t)=\lim_{\epsilon\to 0+}\frac{d}{dt}\frac{1}{2\hbar L^2}\left(\frac{\hbar^2}{2m_I}\right)^3\rho_1^{(I)}(z)\int\frac{d^2q_R}{(2\pi)^2}(\mathbf{q}_R+\mathbf{q}_\parallel)\left|\frac{\mathbf{q}_R\cdot\mathbf{q}_\parallel X_{o,R}(q_R)e^{-\epsilon t}}{\hbar\omega_R(q_R)+\frac{\hbar^2}{2m_I^*}(\mathbf{q}_R+\mathbf{q}_\parallel)^2-\hbar\omega+i\epsilon}\right|^2$$

$$=\frac{1}{\hbar L^2}\left(\frac{\hbar^2}{2m_I}\right)^3\rho_1^{(I)}(z)\mathrm{Im}\int\frac{d^2q_R}{(2\pi)^2}\frac{(\mathbf{q}_R+\mathbf{q}_\parallel)|\mathbf{q}_R\cdot\mathbf{q}_\parallel X_{o,R}(q_R)|^2}{\hbar\omega_R(q_R)+\frac{\hbar^2}{2m_I^*}(\mathbf{q}_R+\mathbf{q}_\parallel)^2-\hbar\omega-i\epsilon}. \tag{4.2}$$

Due to symmetry, the total decay rate can only be in the direction $\mathbf{q}_\parallel$ of the current. The decay rate relative to the elastic current

$$\mathbf{j}^{(I)}_{2,\mathrm{el}}(\mathbf{r};t)=\frac{\hbar}{m_IL^2}\rho_1^{(I)}(z)\mathrm{Im}\left[\sqrt{\rho_1^{(I)}(\mathbf{r})}\,\eta_0^*(\mathbf{r})\,\nabla\frac{\eta_0(\mathbf{r})}{\sqrt{\rho_1^{(I)}(\mathbf{r})}}\right]$$

$$=\frac{\hbar\mathbf{q}_\parallel}{m_IL^2}\rho_1^{(I)}(z) \tag{4.3}$$

is then

$$\frac{1}{\tau}=\frac{1}{|\mathbf{j}^{(I)}_{2,\mathrm{el}}(\mathbf{r};t)|}\lim_{\epsilon\to 0+}\frac{d}{dt}|\mathbf{j}^{(I)}_{2,\mathrm{inel}}(\mathbf{r};t)|$$

$$=\frac{1}{2q_\parallel}\left(\frac{\hbar^2}{2m_I}\right)^2$$

$$\times\mathrm{Im}\int\frac{d^2q_R}{(2\pi)^2}\frac{(q_\parallel+\mathbf{q}_R\cdot\hat{\mathbf{q}}_\parallel)|\mathbf{q}_R\cdot\mathbf{q}_\parallel X_{o,R}(q_R)|^2}{\hbar\omega_R(q_R)+\frac{\hbar^2}{2m_I^*}(\mathbf{q}_R+\mathbf{q}_\parallel)^2-\hbar\omega-i\epsilon}. \tag{4.4}$$

The calculation is somewhat tedious and complicated especially if the effective mass is different from the bare mass. Defining the ratio between the electron thermal velocity and the speed of third sound, $\lambda=m_I^*c_3/\hbar q_\parallel=c_3/v_e$, where $v_e=\hbar q_\parallel/m_I^*$ is the electron velocity, the leading term in λ^{-1} is

$$\frac{1}{\tau}=\frac{1}{6\pi}\left(n\frac{d\mu_I}{dn}\right)^2\left(\frac{m_I^*}{m_4}\right)^2\frac{m_4}{\hbar^2n}\frac{1}{\lambda}+\mathcal{O}(\lambda^0)$$

$$=\frac{1}{6\pi}\left(n\frac{d\mu_I}{dn}\right)^2\left(\frac{m_I^*}{m_4}\right)^2\frac{m_4}{\hbar^2n}\frac{v_e}{c_3}+\mathcal{O}(\lambda^0). \tag{4.5}$$

In the case $m_I^*=m_I$, one obtains the following less complicated result that is valid for all $\lambda<1$:

$$\frac{1}{\tau}=\frac{1}{6\pi}\left(n\frac{d\mu_I}{dn}\right)^2\left(\frac{m_I}{m_4}\right)^2\frac{m_4}{\hbar^2n}\left[\frac{\sqrt{1-\lambda^2}(1+2\lambda^2)}{\lambda}-\frac{3\pi}{2}+3\arcsin\lambda\right]. \tag{4.6}$$

This expression gives the dependence of the decay rate on the essential physical parameters. Our result is the ratio of two terms that go to zero in the limit of thick films. The third sound mode with velocity c_3 will eventually turn into a ripplon mode with the familiar $q_\parallel^{3/2}$ dispersion relation for which our theory does not apply. Also, the electron chemical potential should approach a constant in the thick-film limit. One expects, however, that the dependence of the electron chemical potential as a function of film thickness is relatively smooth, whereas the third sound speed is known to oscillate strongly.[27,29]

The above calculation has omitted all but the transitions in the lowest states, and has employed throughout long-wavelength expansions. Our final result shows why this is justified: other terms in the self-energy or the current would describe coupling to higher-lying states. One may expect that they contribute a smooth background correction, but the appearance of the third sound speed in the denominator is responsible for the characteristic oscillations of the lifetime and, hence, of the electron mobility.

V. RESULTS

A. Substrate model

In this work, both the substrate and the helium films are treated as homogeneous systems with individual dielectric constants ϵ_S for the substrate and ϵ_H for ^{4}He. We assume a ^{4}He film of thickness $h=n/\rho_\infty$ whose surface is at $z=0$ and a flat substrate half space between $-\infty<z<-h$. The potential seen by the electron is then[34]

$$U_{\mathrm{sub}}(z)=\begin{cases}\infty & \text{for } z\leqslant 0\\ \dfrac{\xi_{VH}e^2}{4z}+\dfrac{e^2}{4}\dfrac{\xi_{VH}^2-1}{\xi_{VH}}\displaystyle\sum_{n=1}^{\infty}\frac{(\xi_{VH}\xi_{SH})^n}{z+nh} & \text{for } z>0,\end{cases} \tag{5.1}$$

where

$$\xi_{VH}=\frac{1-\epsilon_H}{1+\epsilon_H}\ \text{and}\ \xi_{SH}=\frac{\epsilon_S-\epsilon_H}{\epsilon_S+\epsilon_H}. \tag{5.2}$$

The hard core for the helium potential barrier is a reasonable model because the measured potential barrier seen by the electron at the ^{4}He surface is about 1 eV.[1]

As the film thickness increases, the binding energy of the electron varies between the binding energy of the electron on the bare substrate and the one on a helium half space. Since the binding on the ^{4}He half space is much weaker than on the substrate, the electron will, with increasing film thickness, also move away from the surface.

Figure 1 shows the dependence of the electron binding energy and the distance of the electron from the ^{4}He surface

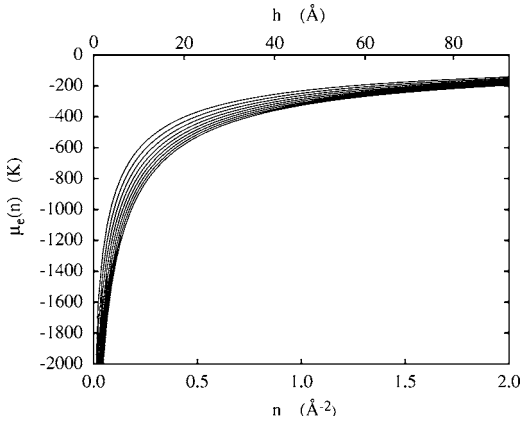

FIG. 1. The figure shows the electron binding energy $\mu_e(n)$ as a function of surface coverage n (lower scale) and film height h (upper scale). The curves correspond to the substrate dielectric constant $\epsilon_S=3,3.25,3.5,\ldots,5$ from top to bottom.

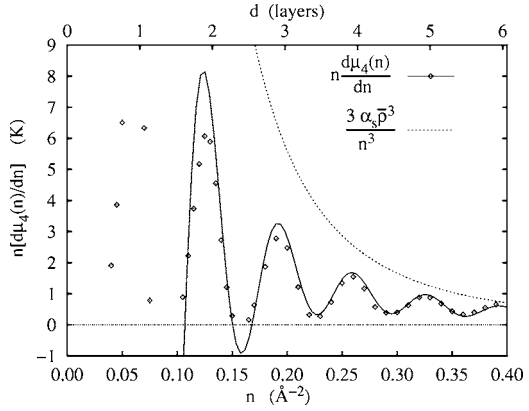

FIG. 2. The figure shows the calculated incompressibilities $m_4c_3^2$ of ^{4}He on the glass substrate as calculated from the long-wavelength limit of the excitations (diamonds). Also shown are the results obtained by differentiating the fit [Eq. (5.3)] (solid line) and the asymptotic form $mc_3^2(n)\approx 3\alpha_s\bar{\rho}^3/n^3$ for large n (short-long dashed line). The upper scale gives the thickness of the ^{4}He films in units of *liquid layers.* We have defined here the thickness of one layer from the value k of the fit [Eq. (5.3)], with the number d of layers as $d=0.066n$, which is somewhat less than the experimental relationship $d=0.077n$. (Results from Ref. 27).

as a function of ^{4}He film thickness. For the computation, we have assumed a range of substrate dielectric constants of $3\leqslant\epsilon_S\leqslant 5$ and a ^{4}He dielectric constant of $\epsilon_H=1.055$. The values of the substrate dielectric constants model a glass substrate as described in the following subsection. The film was modeled as having constant density over a width h, which was converted to ^{4}He coverage n. In the limit of zero film thickness, the binding energy to the substrate varies between −4400 and −2500 K. In the limit of infinite film thickness the binding energy approaches −7.12 K and the distance from the ^{4}He surface is over 80 Å. From Fig. 1, it is seen that even a film of nominal thickness 100 Å is far from the bulk half-space limit. Thus, the influence of the substrate reaches far into the regime where the ^{4}He film would otherwise be considered as "bulk." This observation is relevant because it demonstrates that thick-film approximations should not be used to estimate the term $d\mu_I/dn$ in Eq. (3.15) and (4.5).

B. Helium films and third sound

Recently, we have reported very extensive studies of the dependence of the ^{4}He third sound speed as a function of both the nature of the substrate and the film thickness.[27] For films up to a coverage of 0.4 Å^{-2}, we have fitted the ^{4}He chemical potential $\mu_4(n)$ by a function

$$\mu_4(n)=\mu_4(\infty)-\frac{\alpha_s\bar{\rho}^3}{n^3}+\frac{c}{n^4}+\frac{d}{n^5}+\frac{e\cos(kn-\gamma)}{n^4}, \quad (5.3)$$

where α_s is the van der Waals constant of the substrate and $\bar{\rho}$ is an average density. We have derived from this fit, as well as from the microscopic calculation of the speed of third sound, values for the incompressibility $m_4c_3^2=n(d\mu_4/dn)$. We base the calculations of this work on our results for a glass substrate. The relevant parameters are[27] $\alpha_s=1260$ K Å^3, $\bar{\rho}=.0228$ Å^{-3}, $k=94.43$ Å^2, $c=2.17\times10^{-3}$ K Å^{-8}, $d=-0.89\times10^{-4}$ K Å^{-10}, $e=1.20\times10^{-4}$ K Å^{-8}, and $\gamma=1.27$. These parameters were derived from calculations for helium films of six to seven layers.

Figure 2 shows the surface incompressibility of ^{4}He on the glass substrate as calculated in Ref. 27. The strong oscillations as a function of coverage are characteristic of third sound in thin ^{4}He films. Note also that the "hydrodynamic limit," as described by the van der Waals form for the ^{4}He chemical potential, is far from being reached.

Of course, one must be cautious when extrapolating the fit [Eq. (5.3)] to films that are much thicker than the regime from which the results were obtained; we have therefore used in our calculations a conservative extrapolation of our fit [Eq. (5.3)] up to a coverage of $n=0.6$ Å^{-2}, corresponding to about nine layers.

C. Electron mobility

From the data on the energetics of electron bound states and the ^{4}He third sound speed, we can calculate the effective-mass ratio [Eq. (3.15)] and the contribution of the ^{4}He film to the loss rate [Eq. (4.5)] of the thermal electrons and, from that, the electron mobility

$$\mu=\frac{e}{m_I}\tau. \quad (5.4)$$

A quantitative calculation of the ^{4}He contribution to the electron effective mass and the mobility is evidently delicate because these quantities depend on the ratio of two quantities, $n(d\mu_I/dn)$ and c_3, that both go to zero in the thick-film limit. One expects that the electron binding energy is relatively insensitive against the layer structure, because it is dominated, for thin films, by the substrate and layering effects in the density profile are negligible for film thicknesses of more than three or four layers. On the other hand, the speed of third sound shows, for practically all substrates, the pronounced oscillation seen in Fig. 2.

The primary quantities to calculate are the effective-mass ratio [Eq. (3.15)] and the damping rate $1/\tau$ [Eq. (4.5)]. The

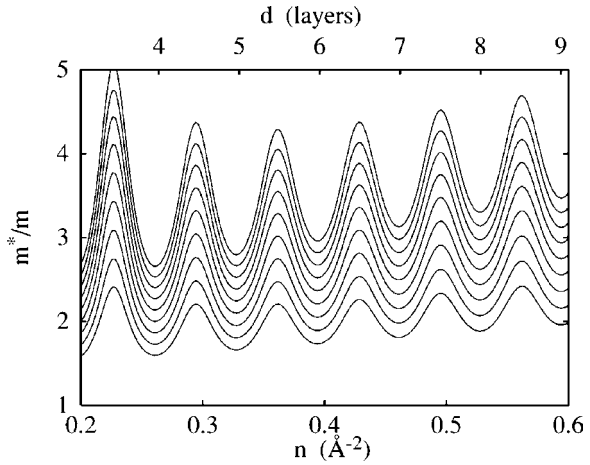

FIG. 3. The figure shows the contribution of the ^{4}He film to the electron effective-mass obtained from solving Eq. (3.15) self-consistently as a function of ^{4}He coverage n for the substrate dielectric constants $\epsilon_S=3,3.25,\ldots,5$. The strongest substrate corresponds to the largest effective mass.

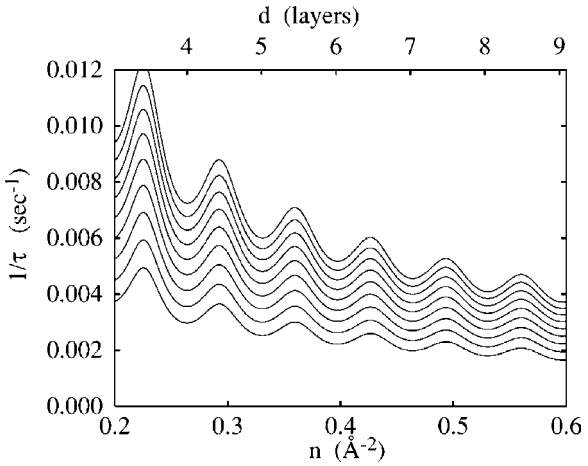

FIG. 4. The figure shows the contribution of the ^{4}He film to the electron-energy-loss rate calculated from Eq. (4.5) as a function of ^{4}He coverage n (solid line, left scale) for the substrate dielectric constants $\epsilon_S=3,3.25,\ldots,5$. The strongest substrate corresponds to the largest decay rate.

generic equation [Eq. (3.15)] has been used quite successfully[30] to predict the effective mass of ^{3}He and hydrogen isotope impurities in the surface of ^{4}He. The situation here is different in the sense that we are looking at much thicker films where, due to the fact that the speed of third sound goes to zero, a single term becomes dominant. Figure 3 shows the effective-mass ratio m_1^*/m_1 as a function of coverage for the family of substrate dielectric constants mentioned above. Without the last term in square brackets in Eq. (3.15), the effective-mass ratio can come out negative, and one must therefore solve the equation self-consistently. We find that the electron effective mass depends relatively sensitively on the substrate strength and can be as large as 5 for $\epsilon_S=5$. We note that this effect is present even in the absence of substrate periodicity or defects. Figure 3 shows that for thin ^{4}He films, this behavior depends largely on the magnitude of the dielectric constant of the substrate. A less polarizable substrate, or a more highly compressed ^{4}He film with a larger speed of sound, can cause effective mass ratios that are much closer to 1.

Figure 4 shows the decay rate $1/\tau$. For our calculations, we have assumed a thermal speed of the electrons of $v_e=5000$ m/s. To be able to separate the influence of the effective-mass ratio and the speed of third sound, these results do *not* contain the electron-effective-mass ratio that appears in Eq. (4.5). We see again pronounced oscillations that are obviously due to the oscillations of the third sound speed.

It appears that the two terms, $(nd\mu_1/dn)^2$ and c_3, go to zero at about the same rate, and the chemical potential term falls off slightly faster. This leaves the decay rate oscillating with roughly the same amplitude and a rather slow decay. In the effective-mass ratio, the third sound speed appears squared in the denominator; hence, the oscillations increase with increasing coverage.

VI. CONCLUSION

In this paper, we have calculated the inelastic-scattering rate for an electron on ^{4}He film surfaces up to nine atomic layers on a model glass substrate. Our major result, Eq. (4.6), is a first-principles microscopic derivation of the scattering rate due to coupling to third sound (ripplons). We have identified the term that is responsible for the behavior of the flux decay rate and, consequently, for an electron mobility that oscillates synchronously with layer formation of the underlying helium film. The reasons for this oscillatory behavior is the dependence of the third sound speed on the layered structure of the film and the appearance of that third sound speed in the denominator of the decay rate. This causes oscillations whose amplitude does not appear to decay rapidly with the film thickness.

We do not claim here that transitions to higher-lying excitations are completely negligible; however, we have identified the oscillatory term. Other corrections can, at most, contribute a smooth background of the same order of magnitude. Thus, the dominant contribution to the mobility is shown to depend explicitly on the ratio of the third sound speed to the average electron speed and also the derivative of the electron chemical potential with respect to the film coverage. The third sound speed oscillates synchronously with ^{4}He layer formation, but the electron chemical potential is a smooth function. Thus, we have shown explicitly that, in agreement with experiment,[15,16] the electron mobility on thin ^{4}He films should exhibit oscillations in concert with layer formation.

When the scattering rate shown in Fig. 4 is turned into a mobility via Eq. (5.4), (cf. Fig. 5), we find results on the order of 10^2 m^2/V s corresponding to the smallest values of the dielectric constant. These results are roughly two orders of magnitude larger than the reported electron mobilities on thin helium films.[15,16] It is our understanding that the mechanism suggested by Monarkha *et al.*[21] is at work and the existing two thin-film measurements of electron mobilities have been dominated by scattering due to substrate surface impurities and inhomogeneities. In Ref. 21, the authors report, at their lowest temperature, a 2 orders of magnitude increase in the electron mobility on a hydrogen substrate by

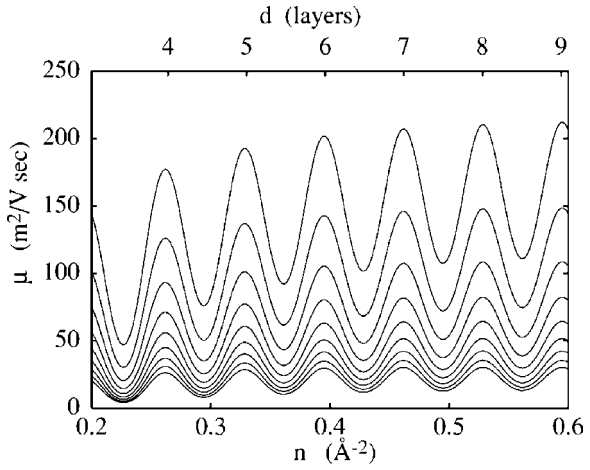

FIG. 5. The figure shows the contribution of the ^{4}He film to the electron mobility, calculated from Eq. (5.4) as a function of ^{4}He coverage n (solid line, left scale) for the substrate dielectric constants $\epsilon_S=3,3.25,\ldots,5$. The effective-mass ratio $(m^*/m)^2$ appearing in Eq. (4.5) is included in these results; the results with the lowest mobility correspond to the largest substrate dielectric constant. Note that the mobility μ should not be confused with the ^{4}He chemical potential μ_4 or the electron binding energy μ_I.

simply annealing the substrate. Further theoretical support is found in Refs. 23 and 24.

We specifically point out the fact that the experiments of Refs. 15 and 16 show small mobility oscillations on top of a smooth background, whereas our results of Figs. 4 and 5 indicate that the oscillations of the mobility due to *coupling* to the ^{4}He film are in size comparable to the total scattering rate off the helium film. Experiments indicate (a) that the oscillatory terms are a small correction on a smooth background and (b) that the background contribution can be changed by orders of magnitude by annealing the substrate. We therefore conclude that we have identified the essential cause of the mobility oscillations as being due to the form [Eq. (4.5)] of the helium-induced flux loss rate. Moreover, although we started from a highly sophisticated and manifestly microscopic many-body description of the compound dynamical system, we have arrived at plausible working formulas for the dominant terms that depend only on physical observables.

To conclude, we should mention the findings by Paalanen and Iye[15] and by Cieslikowski *et al.*[35] (Fig. 9 of Ref. 35) who observe a decrease of the electron mobility with increasing film thickness. In fact, in Ref. 35, the decrease in maximum amplitude as a function of film thickness is shown to follow a power law. This effect is somewhat counterintuitive; it has been interpreted as "due to the stiffening of the film surface caused by the van der Waals term in the ripplon spectrum."[15] However, the ripplon stiffening is one of the outcomes of our description. A possible explanation is the softening of the ripplon mode with increasing film thickness. The limit of our equations [Eq. (4.5)] is delicate since both the numerator and the denominator go to zero and it might well be that the behavior of the mobility as the film thickens depends sensitively on the effects of substrate preparation.

ACKNOWLEDGMENT

M.D.M. would like to express his appreciation to the Institute for Theoretical Physics at Johannes-Kepler University for support during the period of a professional leave.

APPENDIX: THICK-FILM LIMIT

Although the mobility of electrons on an infinite half space of ^{4}He is not the concern of this paper, it is important to examine whether the theory has a well-defined limit. Both the numerator and the denominator of the effective-mass ratio [Eq. (3.15)] and the damping rate [Eq. (4.5)] go to zero in the thick-film limit. However, the physical mechanisms are different: the numerator term $(nd\mu_I/dn)^2$ depends on the interaction of the electron with the substrate, whereas the denominator term is determined by the helium-substrate interaction and the *internal* structure of the helium film.

There are three basic differences between films of finite thickness and the thick-film limit. First, in that limit, the third sound speed c_3 appearing in the denominator of Eqs. (3.15) and (4.5) goes to zero. At the same time, the regime where the spectrum is linear also shrinks. Instead, the spectrum becomes dominated by the ripplon dispersion relation

$$\omega_r^2(q_R) = \frac{\sigma q_R^3}{m_4 \rho_\infty}, \tag{A1}$$

where ρ_∞ is the bulk density and σ is the surface energy.

Second, the derivative $nd\mu_I/dn$ goes to zero with increasing ^{4}He film thickness. This balances the fact that the speed of third sound also goes to zero. Our numerical calculations indicate that the coverage dependence of the electron chemical potential is extremely slow; even films of 100 Å thickness are far from the asymptotic limit. Similarly, the speed of third sound has not reached its asymptotic limit for those film thicknesses where reliable statements can be made.[36]

Third, the sound modes within the background film become dense and it becomes energetically feasible to also excite sound waves that penetrate into the film, perpendicular to the free surface. These excitations have a *linear* dispersion law and are therefore *above* the ripplon excitation, which should remain the dominant energy-loss mechanism; this is the basic assumption of this section.

For thick films, we can use the interpolation formula[37] for the third-sound (ripplon) dispersion relation,

$$\hbar^2\omega_R^2 = \left(\frac{\hbar^2 c_3^2}{h} + \frac{\hbar^2 q_R^2 \sigma}{m_4 \rho_\infty}\right) q_R \tanh q_R h, \tag{A2}$$

where $h=n/\rho_\infty$ is the average height of the film. The shape of the long-wavelength density oscillation in an infinite half space follows directly from Eq. (3.6),

$$\frac{d}{dn} \to -\frac{1}{\rho_\infty}\frac{d}{dz} \quad \text{as } n \to \infty. \tag{A3}$$

Only the momentum-dependent normalization factor depends on the dispersion relation, and thus[33]

$$\phi_R(z) = -\sqrt{\frac{2\rho_\infty \hbar q_R \tanh q_R h}{m_4 \omega_R(q_R)}} \frac{d\sqrt{\rho_1(z)}}{dn}. \tag{A4}$$

We keep the coverage dependence of the particle-hole interaction,

$$V_{o,R}(q_R) = -\sqrt{\frac{\rho_\infty \hbar q_R \tanh q_R h}{2m_4 \omega_R(q_R)}} \frac{d\mu_I}{dn} \tag{A5}$$

and determine $X_{r,k_r}(z)$, for small k_r, from Eq. (3.9) as follows:

$$\tilde{X}_{r,q_r}(z) = -\sqrt{\frac{2\rho_\infty \hbar q_R \tanh q_R h}{m_4 \omega_R(q_R)}} \frac{d\mu_I}{dn} \frac{1}{\hbar\omega_R(r_R) + \frac{\hbar^2 q_R^2}{2m_I}}. \tag{A6}$$

We first use this in the effective-mass formula [Eq. (3.15)]. We introduce a new variable $x = hq_R$; with this, the interpolation formula [Eq. (A2)] reads

$$\omega_R^2(q_R) = \left(\frac{3\alpha_s}{m_4 h^4} + \frac{q_R^2 \sigma}{m_4 \rho_\infty}\right) q_R \tanh q_R h = \frac{1}{m_4 h^5}\left(3\alpha_s + \frac{h^2 x^2 \sigma}{\rho_\infty}\right) x \tanh x. \tag{A7}$$

We can also take the asymptotic form $m_4 c_3^2 = 3\alpha_s/h^3$ for the incompressibility. After this change of variables, the expression [Eq. (3.15)] for the effective mass becomes

$$\begin{aligned}
\frac{m_I}{m_I^*} &= 1 - \int_0^\infty \frac{dq_R q_R}{2\pi} |X_{o,R}(q_R)|^2 \frac{\frac{\hbar^2 q_R^2}{2m_I}}{\hbar\omega_R(q_R) + \frac{\hbar^2 q_R^2}{2m_I^*}} \\
&= 1 - \frac{1}{\rho_\infty}\left(\frac{d\mu_I}{dh}\right)^2 \int_0^\infty \frac{dq_R q_R}{\pi} \frac{\hbar q_R \tanh q_R h}{m_4 \omega_R(q_R)} \times \frac{\frac{\hbar^2 q_R^2}{2m_I}}{\left(\hbar\omega_R(q_R) + \frac{\hbar^2 q_R^2}{2m_I^*}\right)^3} \\
&\approx 1 - \frac{1}{\pi m_I m_4 \rho_\infty}\left(\frac{d\mu_I}{dh}\right)^2 \int_0^\infty dq_R \frac{q_R^4 \tanh q_R h}{\omega_R^4(q_R)} \\
&= 1 - \frac{m_4}{2\pi m_I \rho_\infty}\left(\frac{d\mu_I}{dh}\right)^2 h^5 \int_0^\infty dx \frac{x^2}{\left(3\alpha_s + \frac{h^2 x^2 \sigma}{\rho_\infty}\right)^2} \tanh x \\
&\to 1 - \frac{m_4}{2\pi m_I \rho_\infty}\left(\frac{d\mu_I}{dh}\right)^2 h^5 \frac{\rho_\infty}{6\sigma\alpha_s h^2} \quad \text{as } h \to \infty.
\end{aligned} \tag{A8}$$

If $\mu_I(h)$ goes as $1/h$, then the effective-mass correction goes as $1/h$ for large h, i.e., the effective mass goes to m_I in the thick-film limit.

Since the inverse lifetime has one factor of c_3 less in the denominator, it is not necessary to calculate this limit explicitly.

Things change somewhat if we also allow for retardation of the substrate potential. Then, the substrate potential assumes the asymptotic form[38]

$$U_{\text{ext}}(z) \sim \frac{\alpha_s}{z^3(1 + z/\lambda)} \quad \text{as } z \to \infty. \tag{A9}$$

In that case, the effective mass goes to a constant, but the inverse lifetime still goes to zero.

We should, of course, point out that the above half-space limit is never really reached because for thick (saturated) films or the bulk free surface, gravity will eventually take over. The purpose of our exercise was to show that the theory does not have any undesirable divergences in the thick-film limit.

*Electronic address: eckhard.krotscheck@jku.at
†Electronic address: mdm@wsu.edu

[1] W. T. Sommer, Phys. Rev. Lett. **12**, 271 (1964).
[2] M. W. Cole and M. H. Cohen, Phys. Rev. Lett. **23**, 1238 (1969).
[3] M. W. Cole, Phys. Rev. B **2**, 4239 (1970).
[4] T. R. Brown and C. C. Grimes, Phys. Rev. Lett. **29**, 1233 (1972).
[5] W. T. Sommer and D. J. Tanner, Phys. Rev. Lett. **27**, 1345 (1971).
[6] A. S. Rybalko, Y. Z. Kovdrya, and B. N. Esel'son, JETP Lett. **22**, 280 (1975).
[7] C. C. Grimes and G. Adams, Phys. Rev. Lett. **36**, 145 (1976).
[8] F. Bridges and J. F. McGill, Phys. Rev. B **15**, 1324 (1977).
[9] L. P. Gor'kov and D. M. Chernikova, JETP Lett. **18**, 68 (1974).
[10] L. P. Gor'kov and D. M. Chernikova, Sov. Phys. Dokl. **21**, 328 (1976).
[11] M. Wanner and P. Leiderer, Phys. Rev. Lett. **42**, 315 (1979).
[12] H. Ikezi and P. M. Platzman, Phys. Rev. B **23**, 1145 (1981).
[13] H. Etz, W. Gombert, W. Idstein, and P. Leiderer, Phys. Rev. Lett. **53**, 2567 (1984).
[14] K. Kajita and W. Sasaki, Surf. Sci. **113**, 419 (1982).
[15] M. A. Paalanen and Y. Iye, Phys. Rev. Lett. **55**, 1761 (1985).
[16] D. Cieslikowski, A. J. Dahm, and P. Leiderer, Phys. Rev. Lett. **58**, 1751 (1987).

[17] A. Thomy, X. Duval, and J. Regnier, Surf. Sci. Rep. **1**, 1 (1981).
[18] P. A. Crowell and J. D. Reppy, Phys. Rev. Lett. **70**, 3291 (1993).
[19] V. Shikin, J. Klier, I. Doicescu, A. Würl, and P. Leiderer, Phys. Rev. B **64**, 073401 (2001).
[20] K. Shirahama, S. Ito, H. Suto, and K. Kono, J. Low Temp. Phys. **101**, 439 (1995).
[21] Y. P. Monarkha, U. Albrecht, K. Kono, and P. Leiderer, Phys. Rev. B **47**, 13812 (1993).
[22] S. S. Sokolov, J. P. Rino, and N. Studart, Phys. Rev. B **51**, 11068 (1995).
[23] S. Sokolov and N. Studart, Phys. Rev. B **67**, 132510 (2003).
[24] D. Coimbra, S. Sokolov, J. Rino, and N. Studart, J. Low Temp. Phys. **126**, 505 (2002).
[25] V. Apaja and E. Krotscheck, in *Microscopic Approaches to Quantum Liquids in Confined Geometries*, edited by E. Krotscheck and J. Navarro (World Scientific, Singapore, 2002), pp. 205–268.
[26] B. E. Clements, H. Forbert, E. Krotscheck, H. J. Lauter, M. Saarela, and C. J. Tymczak, Phys. Rev. B **50**, 6958 (1994).
[27] E. Krotscheck and M. D. Miller, J. Low Temp. Phys. **141**, 1 (2005).
[28] B. E. Clements, J. L. Epstein, E. Krotscheck, and M. Saarela, Phys. Rev. B **48**, 7450 (1993).
[29] B. E. Clements, E. Krotscheck, and C. J. Tymczak, Phys. Rev. B **53**, 12253 (1996).
[30] B. E. Clements, E. Krotscheck, and M. Saarela, Phys. Rev. B **55**, 5959 (1997).
[31] E. Krotscheck and R. Zillich, Phys. Rev. B **58**, 5707 (1998).
[32] E. Krotscheck and R. Zillich, J. Chem. Phys. **115**, 10161 (2001).
[33] B. E. Clements, E. Krotscheck, and M. Saarela, Z. Phys. B: Condens. Matter **94**, 115 (1994).
[34] K. Kajita, J. Phys. Soc. Jpn. **52**, 372 (1983).
[35] D. Cieslikowski, P. Leiderer, and A. J. Dahm, Can. J. Phys. **65**, 1525 (1987).
[36] E. Krotscheck and M. D. Miller, Phys. Rev. B **73**, 134514 (2006).
[37] R. A. Guyer, M. D. Miller, and J. Yaple, Phys. Rev. B **25**, 4570 (1982).
[38] C. Carraro and M. W. Cole, Prog. Surf. Sci. **57**, 61 (1998), and references therein.